Nanophotonic Computational Design

Jesse Lu* **and Jelena Vučković**
Stanford University, Stanford, California, USA.
jesselu@stanford.edu

Abstract: In contrast to designing nanophotonic devices by tuning a handful of device parameters, we have developed a computational method which utilizes the full parameter space to design linear nanophotonic devices. We show that our method may indeed be capable of designing any linear nanophotonic device by demonstrating designed structures which are fully three-dimensional and multi-modal, exhibit novel functionality, have very compact footprints, exhibit high efficiency, and are manufacturable. In addition, we also demonstrate the ability to produce structures which are strongly robust to wavelength and temperature shift, as well as fabrication error. Critically, we show that our method does not require the user to be a nanophotonic expert or to perform any manual tuning. Instead, we are able to design devices solely based on the user's desired performance specification for the device.

OCIS codes: 230.75370, 130.3990.

References and links

1. Introduction

Currently, almost all nanophotonic components are designed by hand-tuning a small number of parameters (e.g. waveguide widths and gaps, hole and ring sizes). However, the realization of increasingly complex, dense, and robust on-chip optical networks will require utilizing increasing numbers of parameters when designing nanophotonic components.

Opening the design space to include many more parameters allows for smaller footprint, higher performance devices by definition; since original designs are still included in this parameter space. Unfortunately, the lack of intuition for what such designs might look like and the inability to manually search such a large parameter space have greatly hindered the ability to employ anything even close to the available parameter space for designing nanophotonic components.

For this reason, we have developed and implemented a computational method which is able to use the full parameter space to design linear nanophotonic components in three dimensions. Critically, our method requires no user intervention or manual tuning. Instead, a *design-by-specification* scheme is used to produce designs based solely on a user's performance specification.

We show that our method can indeed produce designs which are extremely compact, and, at the same time, highly efficient. Furthermore, we demonstrate that devices with novel functionality are easily designed. We also show that our method can be used to produce designs with extreme robustness to wavelength and temperature shift, as well as fabrication error.

Lastly, since all our results are produced by simply specifying the functionality and performance of the desired device, our results suggest that our method may indeed by able to design *all* linear nanophotonic devices.

2. Problem formulation

In order to produce designs which utilize the full parameter space, and are based solely on the user's performance specification, we formulate the design problem in the following way:

$$\text{minimize} \quad \sum_{i}^{M} \|A_i(z)x_i - b_i\|^2 \tag{1a}$$

$$\text{subject to} \quad \alpha_{ij} \leq |c_{ij}^{\dagger} x_i| \leq \beta_{ij}, \quad \text{for } i = 1,\ldots,M \text{ and } j = 1,\ldots,N_i \tag{1b}$$

$$z_{\min} \leq z \leq z_{\max} \tag{1c}$$

The explanation for the various terms in eq. (1) follows:

1. $A_i(z)x_i - b_i$ is the *physics residual* for the ith mode. That is to say, $A_i(z)x_i - b_i$ represents the underlying physics of the problem; namely, the electromagnetic wave equation $(\nabla \times \mu_0^{-1}\nabla \times -\omega_i^2\varepsilon)E_i + i\omega_i J_i$.

   The specific substitutions used in order to transform

   $$(\nabla \times \mu_0^{-1}\nabla \times -\omega_i^2\varepsilon)E_i + i\omega_i J_i \quad \longrightarrow \quad A_i(z)x_i - b_i$$

   are

   - $E_i \rightarrow x_i$,
   - $\varepsilon \rightarrow z$,
   - $\nabla \times \mu_0^{-1}\nabla \times -\omega_i^2\varepsilon \rightarrow A_i(z)$, and
   - $-i\omega_i J_i \rightarrow b_i$.

   In contrast to typical schemes for optimizing physical structures, our formulation actually allows for non-zero physics residuals; which can be deduced since $A_i(z)x_i - b_i = 0$ is not a hard constraint. Instead, this formulation is what we call an *objective-first* formulation in that the *design objective* (explained below) is prioritized above satisfying physics.

2. The (field) design objective consist of the constraint $\alpha_{ij} \leq |c_{ij}^{\dagger} x_i| \leq \beta_{ij}$. Physically, this constraint describes the performance specification of the device via a series of field overlap integrals at various output ports of the device. Specifically, the $c_{ij}^{\dagger} x_i$ terms represents an overlap integral between the E-field of the ith mode (x_i) with an E-field of the user's choice (c_{ij}), where the additional subscript j allows the user to include multiple such fields. The amplitude of the overlap integral is then forced to reside between α_{ij} and β_{ij}.

   This mechanism allows the user to express the desired performance of the device as a combination of field amplitudes in various output field patterns. These outputs would be in response to a predefined input excitation, which is determined by the current excitation b_i ($-i\omega_i J_i$) in the physics residual of each mode.

   As an example of a design objective for some mode 1 a user might choose to have the majority of the output power reside in some output pattern 1, while ensuring that only a small amount of power be transferred to some output pattern 2. In this case the user

would use $0.9 \leq |c_{11}^{\dagger} x_1| \leq 1.0$ for the former. and then $0.0 \leq |c_{12}^{\dagger} x_1| \leq 0.01$ for the latter; where c_{11} and c_{12} are representative of output patterns 1 and 2 respectively.

Finally, we note again that the design objective in our formulation is actually a hard constraint. This means that it is *always satisfied*, even to the extent of allowing for an unphysical field (since the physics residual will not be exactly 0). It is for this reason that we call such a formulation "objective-first".

3. The final term in eq. (1), $z_{\min} \leq z \leq z_{\max}$, is the structure design objective. It is used as a relaxation of the binary constraint, $z \in z_{\min}, z_{\max}$, which would ensure that the final design be composed of two discrete materials.

3. Method of solution

We employed the alternating directions method of multipliers (ADMM) algorithm in order to solve eq. (1). The ADMM algorithm solves eq. (1) by iteratively solving for x_i, z, and a dual variable u_i.

Since we are working in three dimensions, solving eq. (1) for x_i is non-trivial in that it involves millions of variables and requires solving for the ill-conditioned $A_i(z)$ matrix. For this reason, we use a home-built finite-difference frequency-domain (FDFD) solver which implements a hardware-accelerated iterative solver on Amazon's Elastic Compute Cloud. Critically, our cloud-based solver allows us to scale to solve problems with arbitrarily-large number of modes, with no significant penalty in runtime.

In contrast to solving for x_i, solving for z is much simpler since we only consider planar structures; thereby limiting z to have only thousands of variables.

Lastly, in order to arrive at fully discrete, manufacturable structures, we convert z to a boundary parameterization and tune our structure using a steepest-descent method.

4. Results

We demonstrate the effectiveness of our design method by produce designs for a variety of nanophotonic devices.

All of our results are in three dimensions and consist of a 250 nm etched silicon slab completely surrounded by silica. The permittivity values of silicon and silica used were $\varepsilon_{\mathrm{Si}} = 12.25$ and $\varepsilon_{\mathrm{SiO_2}} = 2.25$ respectively.

Many, if not all, of the produced designs exhibit novel functionality, high efficiency ($> 80\%$), and very compact footprints of only a few square vacuum wavelengths; while still remaining manufacturable. We also show that many devices can be designed to exhibit different functionality for different input excitations. Additionally, we show that devices can be designed with large tolerances for errors in wavelength, temperature and fabrication.

4.1. Mode converters

4.1.1. TE mode converter

Our first result was a mode conversion device operating in the TE polarization, which we define as that mode where the primary E-field component of the waveguide mode is polarized in the plane of the structure. Such a device is significant because it demonstrates the feasibility of muli-mode on-chip optical networks by showing that high-efficiency mode conversion can readily be achieved in planar on-chip nanophotonic structures. Furthermore, this device also demonstrates that this can be achieved within very small device footprints (1.6×2.4 microns for this device in particular).

Our performance specification (fig. 1) for the device was for 90% to 100% of the input power to be transferred from the fundamental waveguide mode, to the second-order waveguide mode. At the same time, we specified that no more than 1% of the input power was to remain in the transmitted fundamental mode.

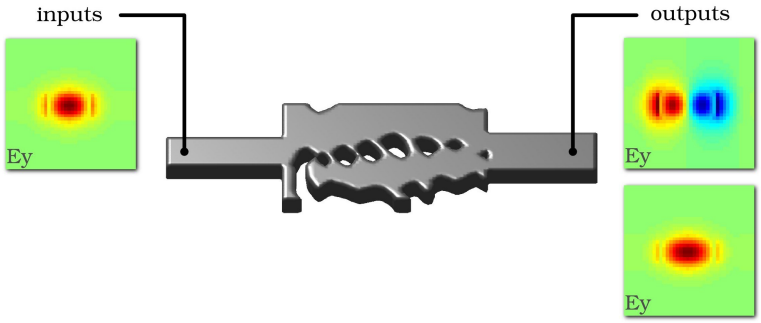

Fig. 1. Perfomance specification of the TE mode converter. Input mode is the fundamental TE-polarized mode on the left. Primary output mode is the second-order mode on the right. Output power in the transmitted fundamental mode on the right above 1% is to be rejected. The structure shown is the final three-dimensional design.

The performance of the device is shown in fig. 2. The conversion efficiency into the second-order mode is lower than desired (86.4% as opposed to 90% to 100%); this may be due to evanescent modes "interfering" with the output field overlap calculation.

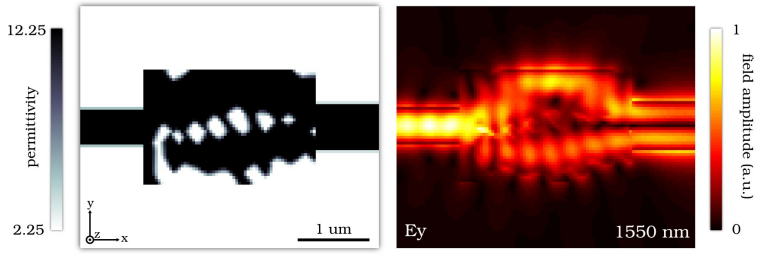

Fig. 2. Structure and E-field at the central plane of the device. The conversion efficiency into the second-order mode is 86.4%, while the power into the rejection mode (fundamental) is 0.7%. Device footprint is 1.6×2.4 microns.

4.1.2. TM mode converter

In addition to mode conversion in the TE polarization (E-field in-plane), we show that TM polarization (E-field out-of-plane) mode converters can be designed as well. This example shows that full three-dimensional structures truly are possible, and that no approximations are needed for our method.

Since our method is design-by-specification, the design of a TM mode converter requires only a small modification to the performance specification of the device; namely the polarization of the input and output modes (fig. 4). Specifically, we still design for $\geq 90\%$ conversion into the second-order mode and a $\leq 1\%$ allowance for the fundamental mode to be transmitted.

The performance of the device is shown in fig. 4. The lower conversion efficiency of 76.9% in contrast to the TE mode converter may be attributed to the lower confinement of the TM

Fig. 3. Perfomance specification of the TM mode converter. Input mode is the fundamental TM-polarized mode on the left. Primary output mode is the second-order mode on the right. Output power in the transmitted fundamental mode on the right above 1% is to be rejected. The structure shown is the final three-dimensional design.

waveguide modes. However, good rejection of only 1% is still achieved.

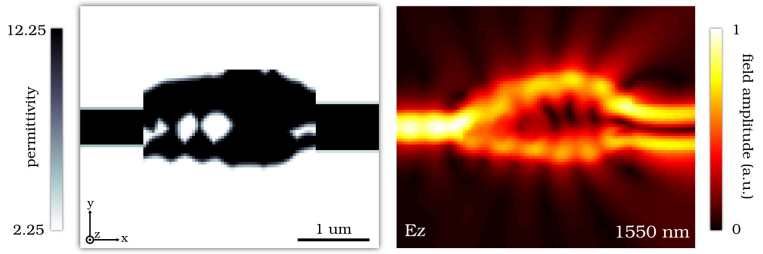

Fig. 4. Structure and E-field at the central plane of the device. The conversion efficiency into the second-order mode is 76.9%, while the power into the rejection mode (fundamental) is 1.0%. Device footprint is 1.6×2.4 microns.

4.2. Splitters

Next, we demonstrate the design of nanophotonic waveguide mode splitters. Such devices can be used as multiplexors or demultiplexors and are the key component in utilizing a single waveguide to transmit multiple optical signals.

As a demonstration of the versatility of our method, we show that it is capable of designing mode splitting devices based on either the spatial profile, the polarization, or the wavelength of the input modes.

The performance specification for each device is simply to convert 90% of the input power in a particular input mode into either one of the output modes. At the same time, we specify that the transmission into the other output mode be kept below 1% of input power.

4.2.1. Spatial mode splitter

We demonstrate what is, to our knowledge, the first design for a three-dimensional nanophotonic spatial mode splitter. Such a device is the key enabler for multi-mode on-chip optical circuits, and we show here that they can be designed to be highly efficient while utilizing a very small device footprint (2.8×2.8 microns). The performance specification is shown in fig. 5, and the final results is shown in fig. 6.

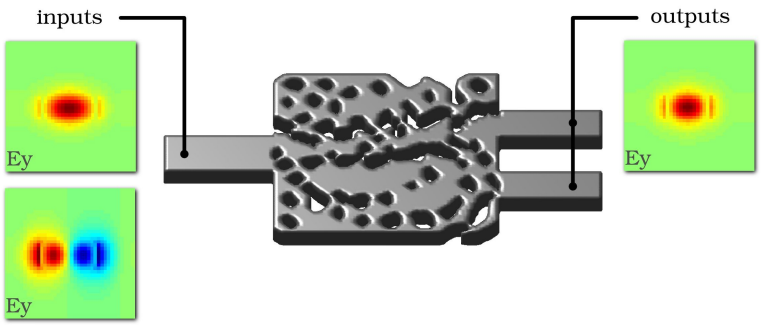

Fig. 5. Input mode is either the fundamental or second-order TE-polarized mode on the left. Output modes are the fundamental waveguide modes of either output waveguide on the right. Output power into the desired output arm is specified to be greater than 90%, while power into the opposing arm is set to below 1%.

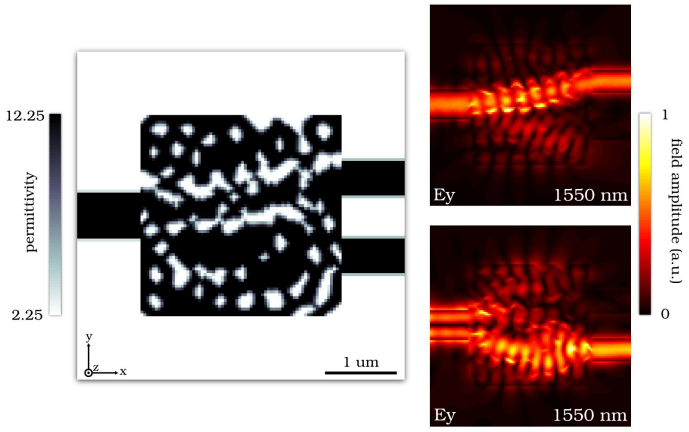

Fig. 6. The conversion efficiencies into the upper and lower output arms are 88.7% and 77.4% respectively, while the rejection powers for the same modes are 0.27% and 0.20%. Device footprint is 2.8×2.8 microns.

4.2.2. TE/TM splitter

In addition to splitting different spatial modes, we show that different polarization can also be split. Fig. 7 shows the performance specification of a device which is able to separate fundamental TE- and TM-polarized waveguide modes into separate arms. The final, verified result is shown in fig. 8.

Not only is this result the first of its kind, it is the first in the device category where a single device is able to control both polarizations within the same device footprint. This shows the versatility and broad applicability of our method.

4.2.3. Wavelength splitter

Traditional wavelength splitting devices can also be designed using our method. Here, we show that the 1550 nm and 1310 nm wavelengths can be split in a very small device footprint (2.8×2.8 microns).

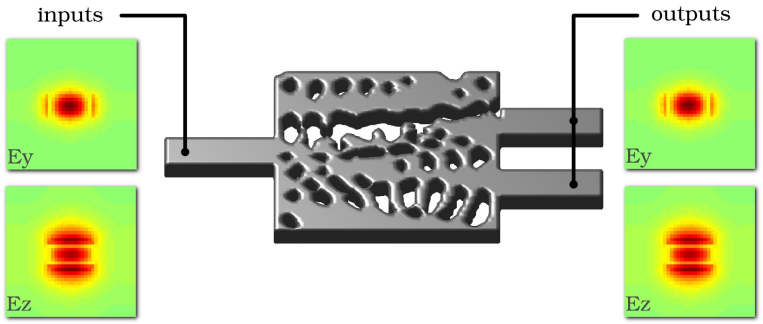

Fig. 7. Input mode is either the fundamental TE- or TM-polarized mode on the left. Output power into the desired output arm is specified to be greater than 90%, while power into the opposing arm is set to below 1%.

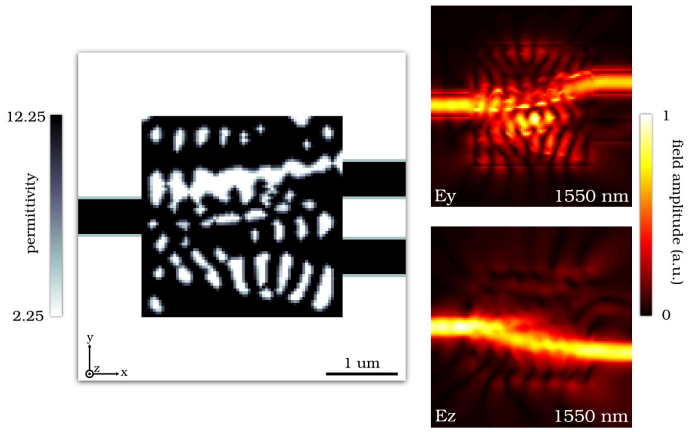

Fig. 8. The conversion efficiencies into the upper and lower output arms are 87.6% and 88.8% respectively, while the rejection powers for the same modes are 1.06% and 0.58%. Device footprint is 2.8×2.8 microns.

Fig. 9. Input mode is the fundamental TE-polarized mode on the left at a wavelength of either 1550 nm or 1330 nm. Output modes are the fundamental waveguide modes of either output waveguide on the right. Output power into the desired output arm is specified to be greater than 90%, while power into the opposing arm is set to below 1%.

5. Conclusion

Conclusion

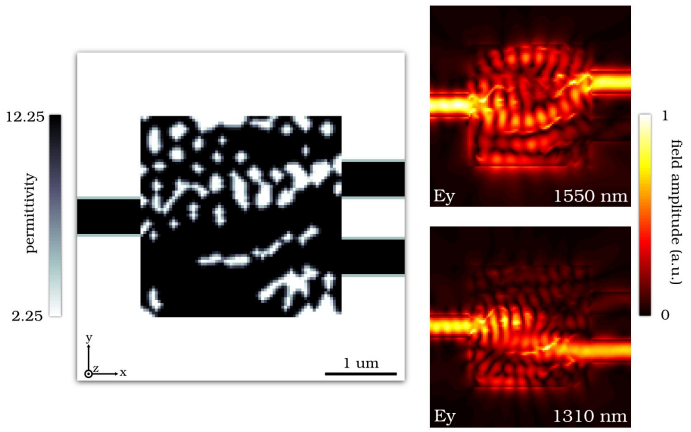

Fig. 10. The conversion efficiencies into the upper and lower output arms are 83.2% and 78.7% respectively, while the rejection powers for the same modes are 0.49% and 1.66%. Device footprint is 2.8×2.8 microns.